Integrated High-Voltage Generators for Low-Power Bistable LCD Drivers

Jan Doutreloigne and Wim Hendrix
University of Gent, ELIS-TFCG/IMEC, Gent, Belgium
Phone: +32-9-2643379, E-mail: jdoutrel@elis.UGent.be

Abstract

This paper describes the architecture, the basic operation principle and detailed experimental results of digitally programmable high-voltage generators that can be used in monolithic low-power high-voltage bistable LCD drivers. Two different design approaches, depending on whether the application allows the use of external passive components or not, are analyzed.

1. Introduction

Modern portable display applications (E-book, PDA, etc.) impose very stringent power consumption restrictions on the display module and its driver circuits. Reflective bistable LCDs, such as cholesteric texture or bistable nematic LCDs, are very interesting candidates for implementation in those portable battery-powered applications because they don't need continuous refreshing to maintain an image on the screen, and hence, they are extremely power-efficient. Their only disadvantage is the relatively high driving voltage (normally between 20V and 100V) needed to switch the pixels from one stable state to the other. As a consequence, these bistable LCDs require dedicated driver chips that combine high-voltage driving capability on one hand and a very low internal power dissipation on the other. Very important for the design of these low-power high-voltage driver chips are the integrated high-voltage generators that convert the battery supply voltage (typically 3V) into digitally programmable high-voltage levels (up to 100V in certain applications) with a high degree of power efficiency. This paper suggests several architectures for the integration of such power-efficient digitally programmable high-voltage generators in advanced smart-power silicon technologies.

2. Results and Discussion

In general terms, the block diagram of a high-voltage display driver looks as in Fig. 1. The two most critical building blocks with respect to power consumption are the level-shifters, responsible for controlling the gate electrodes of the output transistors in the high-voltage analog multiplexers, and the digitally programmable high-voltage generators whose power efficiency has a direct influence on the power dissipation of the entire driver chip. Several architectures and the corresponding electrical performance of the digitally programmable high-voltage generators will be discussed in this section. Special attention will be paid to the choice of charge-pump configuration on the basis of the imposed system specifications.

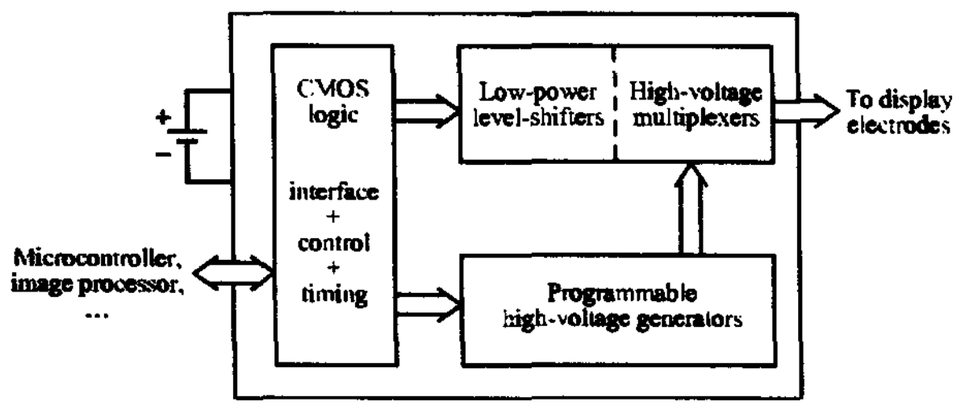

Figure 1: Block diagram of a high-voltage driver.

2.1 Selection of the Charge-Pump

The choice of a specific configuration for the charge-pump, which is the heart of the high-voltage generator, depends on several criteria, such as the maximum desired output voltage and current, the maximum allowed silicon area, the specified power efficiency, and the required response time among others. If output voltages above 50V and output currents in excess of 50μA are needed, the use of external passive components becomes unavoidable in order to keep the silicon area within reasonable limits. In that case, maximum power efficiency can be achieved by adopting a charge-pump architecture where the energy transfer from the low-voltage to the high-voltage side is accomplished by means of an external low-loss inductor. For the control and programming of the output voltage in this type of charge-pump, the architecture of Fig. 2 is suggested. A set of 8 digital input bits transform an internal reference voltage into 1 out of 256 linearly distributed current

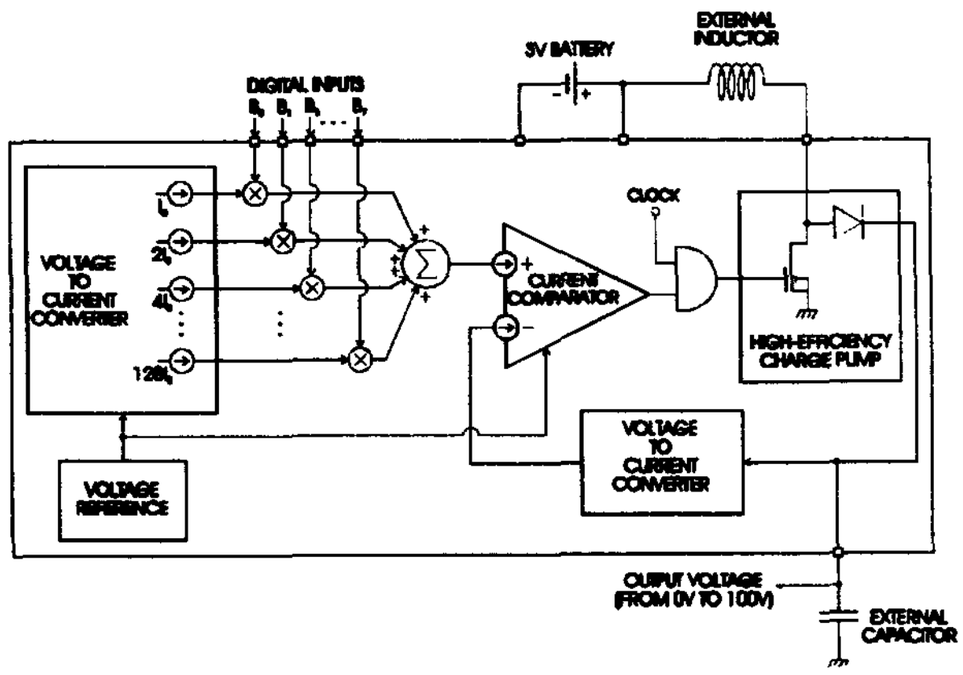

Figure 2: Programmable high-voltage generator based on an external low-loss inductor.

levels. This current level is then compared to a second current level that is proportional to the generator's output voltage. Depending on which of the 2 currents is the largest, the clock signal of the inductor-based charge-pump is enabled or disabled, thereby causing the generator's output voltage to rise or drop. By means of the negative feedback, a situation is reached where the 2 internal current levels become nearly equal, and the output voltage will start to oscillate around a certain mean value with a very small amount of ripple. In this way, 256 linearly distributed voltage levels can be generated.

When the application does not allow the use of external passive components, it is necessary to select another type of charge-pump employing small on-chip capacitors for the energy transfer from the low-voltage to the high-voltage side. However, to keep the silicon area of the capacitor-based charge-pump somewhat acceptable, the maximum achievable output voltage and output current are approximately 50V and 50μA respectively. For the implementation of the fully integrated capacitor-based charge-pump, two fundamentally distinct configurations can be identified: the Dickson and the Makowski charge-pumps as shown in Figs. 3 and 4. In the Dickson type, diodes ensure the correct energy flow on the rhythm of 2 clock signals with a 180° phase shift, while the Makowski type employs switches controlled by 2 non-overlapping clock signals. From a theoretical point of view, the Makowski charge-pump should have a better performance

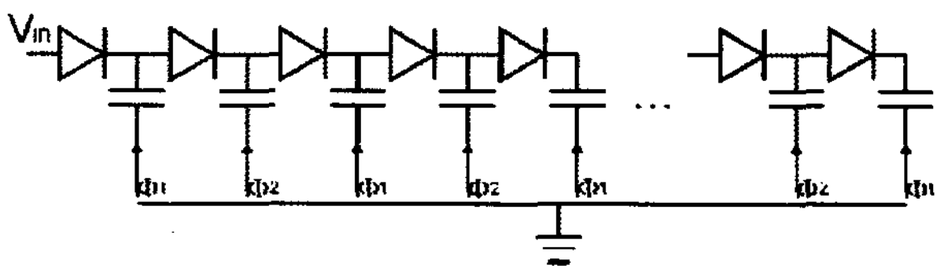

Figure 3: Dickson charge-pump.

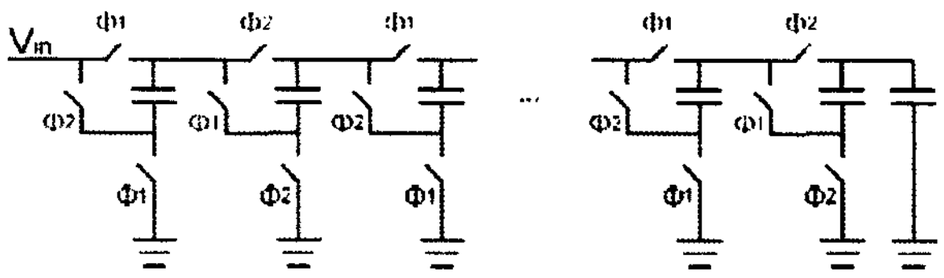

Figure 4: Makowski charge-pump.

because it requires less stages for a given output voltage and it doesn't waste any power in diodes, but the situation is quite different in reality. In actual high-voltage technologies, it turns out that the level-shifters for controlling the high-voltage analog switches in the Makowski charge-pump are constantly discharging the on-chip capacitors, thereby reducing the power efficiency to an unacceptably low value. As a consequence, only the Dickson configuration is of real practical interest for fully integrated high-voltage generators. The most adequate way to program the output voltage of the fully integrated Dickson charge-pump is by means of the control loop depicted in Fig. 5. In this feedback system, the abrupt on/off regulation of the clock signal

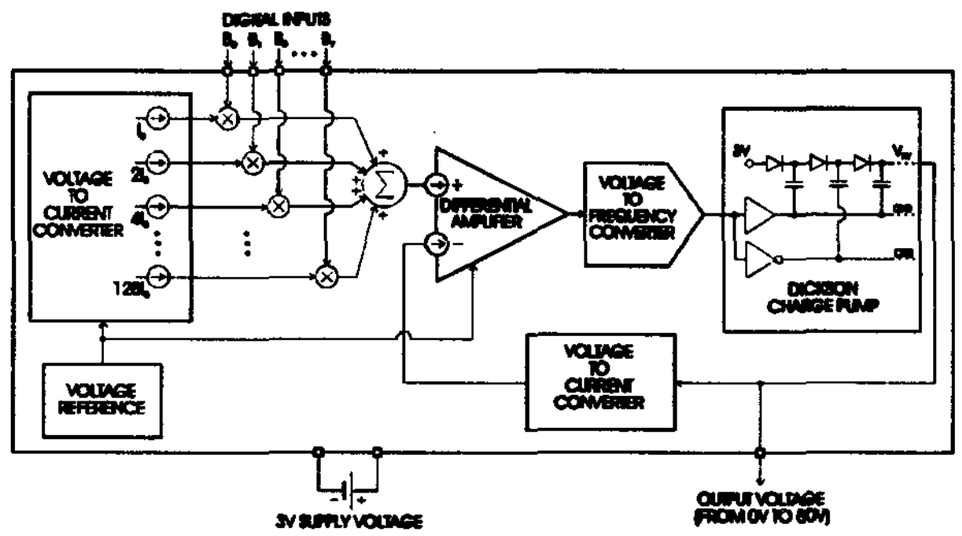

Figure 5: Programmable high-voltage generator based on a fully integrated Dickson charge-pump.

in the charge-pump of Fig. 2 has been replaced by a linear clock frequency regulation. By means of a voltage-to-frequency converter, the clock frequency is continuously adjusted to maintain the 2 current levels at the input of the differential amplifier almost equal. Experiments revealed that the very high clock frequency, required by the Dickson charge-pump to achieve sufficiently high output voltage levels, in combination with the highly ohmic feedback resistor in the voltage-to-current converter connected to the output, result in excessive ripple and overshoot on the output voltage when the abrupt on/off regulation as in Fig. 2 is used. This effect is much less pronounced if a linear clock frequency regulation as in Fig. 5 is used, at the expense of an increased dependence of the output voltage on output current variations.

2.2 Measurements

The programmable high-voltage generator from Fig. 2 was successfully integrated into a low-power 100V driver chip, powered by a tiny 3V battery, for addressing an 80x104 passive matrix cholesteric texture LCD embedded in a sophisticated wrist-watch to allow a preview of pictures taken by a built-in camera [1]. As sudden peak currents of 100μA at output voltage levels up to 100V were required in this advanced application, the high-voltage generator architecture of Fig. 2 was selected with a 220μH low-loss external inductor and a 128 kHz clock frequency with 75% duty ratio for the charge-pump. The accuracy of this generator's programming capability can be observed in Fig. 6, indicating that the absolute non-linearity error of the output

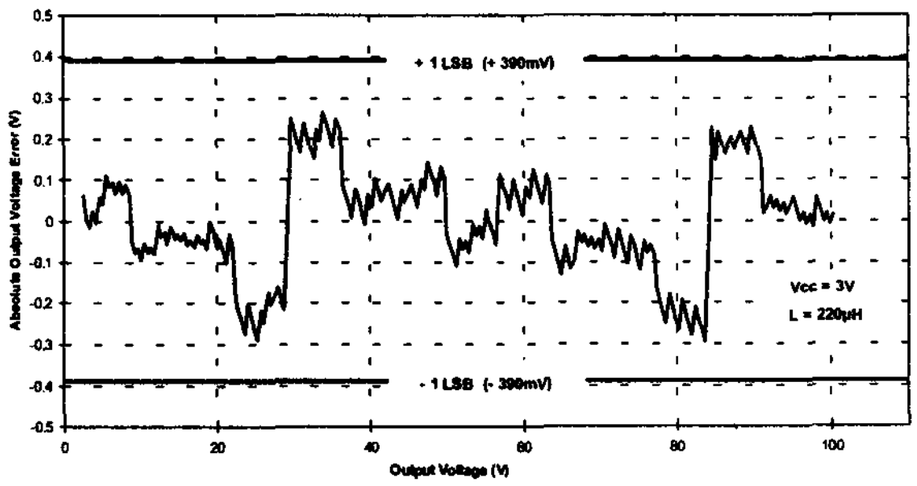

Figure 6: Measured non-linearity error of a high-voltage generator with external inductor.

voltage is less than ±1 LSB at all times. The output current driving capability of the generator for different programmed output voltages is illustrated in Fig. 7. At an output voltage of 100V, the generator is capable of delivering 180μA into the load. At lower output voltages, the maximum output current increases rapidly (e.g. 750μA at 50V). Another very important figure of merit of the high-voltage generator is its power efficiency. In Fig. 8, the measured power efficiency is plotted against the output current for different values of the programmed output voltage. At 100μA output current, a power efficiency of 48% is achieved at 50V output voltage, and still 32% at 100V. This is a very good result in view of the extremely high transformation ratio from 3V to 100V. The dependence of the voltage-vs.-current characteristic on supply voltage variations can be observed in Fig. 9. Apparently, the maximum output current that can be delivered by the generator increases drastically for increasing supply voltages (e.g. from 200μA at Vcc = 2.75V to 550μA at Vcc = 3.25V at an

output voltage level of 75V). It is also seen that the supply voltage variations only have a minor effect on the resulting output voltage level below the maximum output current. However, the power supply rejection can be improved even more by replacing the currently implemented V_T voltage reference by a more stable and reproducible bandgap reference.

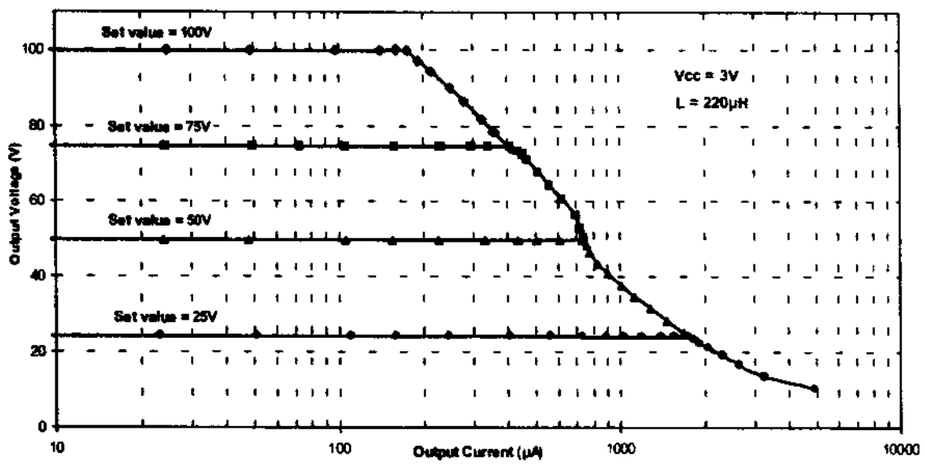

Figure 7: Measured output characteristics of a high-voltage generator with external inductor.

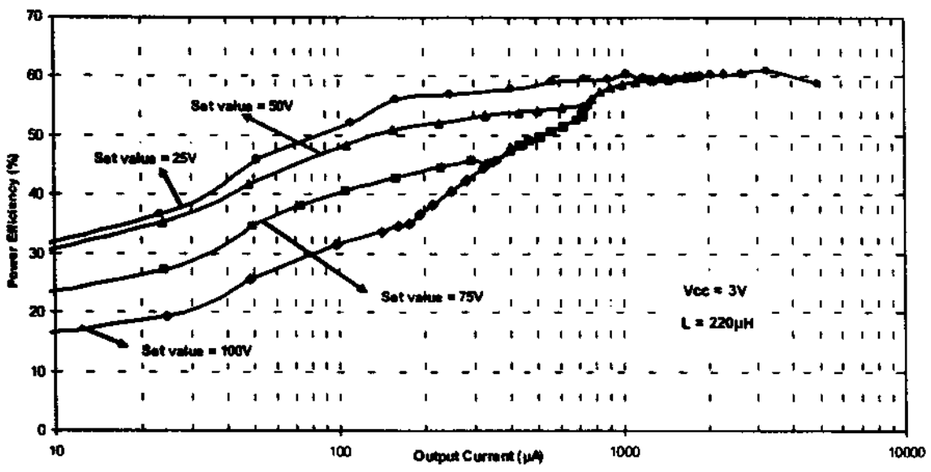

Figure 8: Measured power efficiency of a high-voltage generator with external inductor.

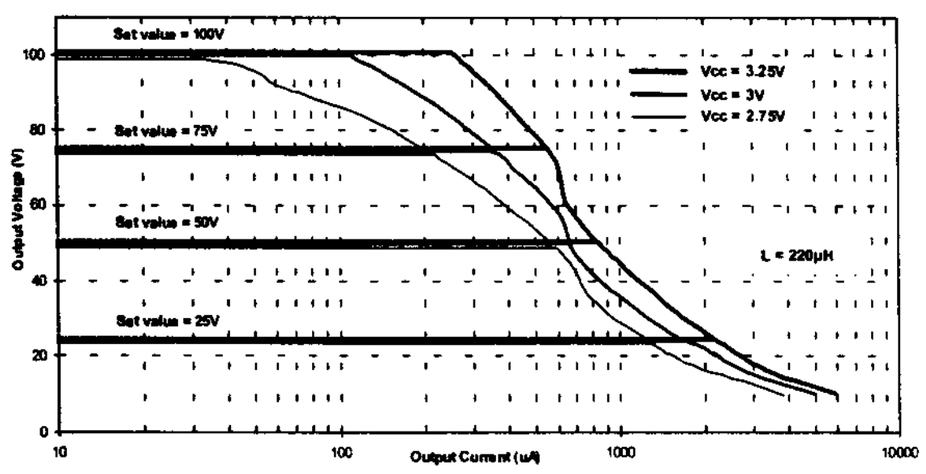

Figure 9: Effect of supply voltage variations on the output characteristics of a high-voltage generator with external inductor.

The programmable high-voltage generator with the fully integrated capacitor-based Dickson charge-pump from Fig. 5 was implemented in a low-power 50V driver chip for addressing a 5-digit 7-segment bistable nematic LCD on a smartcard for electronic purse and electronic ticketing applications [2]. As the smartcard did not allow external passive components, the high-voltage generator architecture of Fig. 5 was indeed the most appropriate choice. To fulfill the design specifications (output currents up to 20µA at 50V output voltage), a 34-stage Dickson charge-pump was implemented with a 10pF high-voltage capacitor in each stage. Clock frequencies up to 10MHz were necessary to deliver enough output current. The total silicon area of this fully integrated programmable high-voltage generator is approximately 4.4mm^2 in an intelligent interface technology based on a 0.7µm CMOS process. The programming capability of this type of generator can be analyzed in Fig. 10, showing the output voltage as a function of the digital input (ranging from 0 to 255) for different load conditions. This graph clearly demonstrates that the output voltage is a linear function of the 8-bit digital input until it saturates at a level that corresponds to the maximum clock frequency produced by the voltage-to-frequency converter. The output voltage level at which this phenomenon occurs depends on the impedance of the load connected to the generator's output. In Fig. 11, the power efficiency of this generator is plotted as a function of the output voltage for different load conditions. Apparently, the maximum achievable power efficiency is about 8.5%. This may seem a rather low value, but this is not surprising in view of the fact that this generator employs only on-chip capacitors. The parasitic capacitance between the bottom

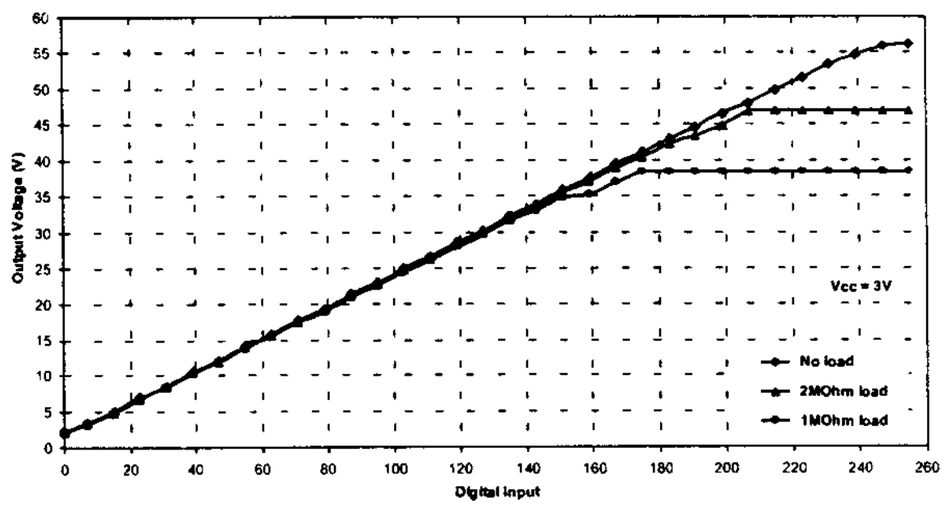

Figure 10: Measured output voltage of a high-voltage generator with a fully integrated Dickson charge-pump.

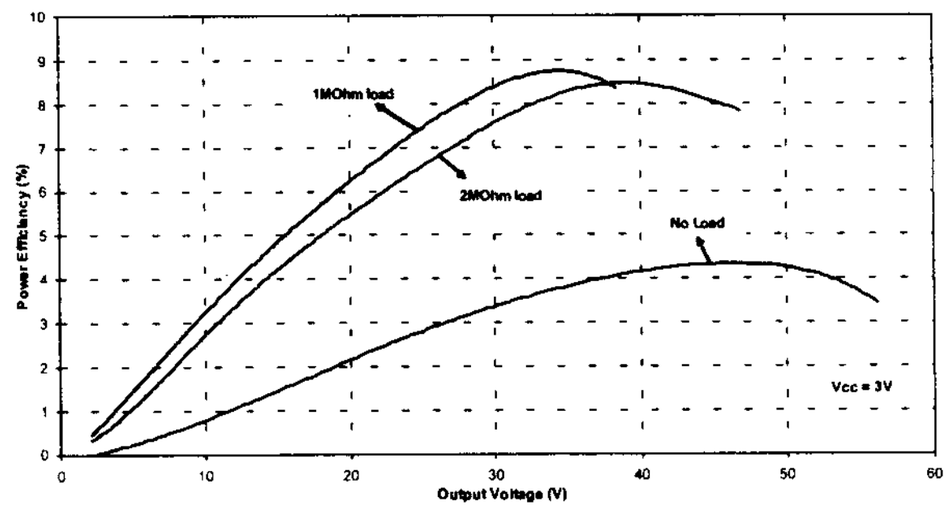

Figure 11: Measured power efficiency of a high-voltage generator with a fully integrated Dickson charge-pump.

electrode of these on-chip capacitors and the substrate (connected to ground) is the main cause of the drastic reduction in power efficiency. In future designs, the effect of this parasitic capacitance will be partially eliminated by using special charge-recycling techniques. A possible implementation of this technique is shown in Fig. 12. After disabling the clock buffer of a specific stage in the charge-pump and before activating the clock buffer of the next stage, the bottom plates of the capacitors in the 2 stages are short-circuited for a moment. In this way, part of the charge stored on the parasitic capacitance between the bottom plates and ground can be recovered, resulting in improved power efficiency.

This is illustrated in the simulation of the generator's supply current during ramp-up in Fig. 13, showing that the charge-recycling yields indeed a supply current reduction of about 25%.

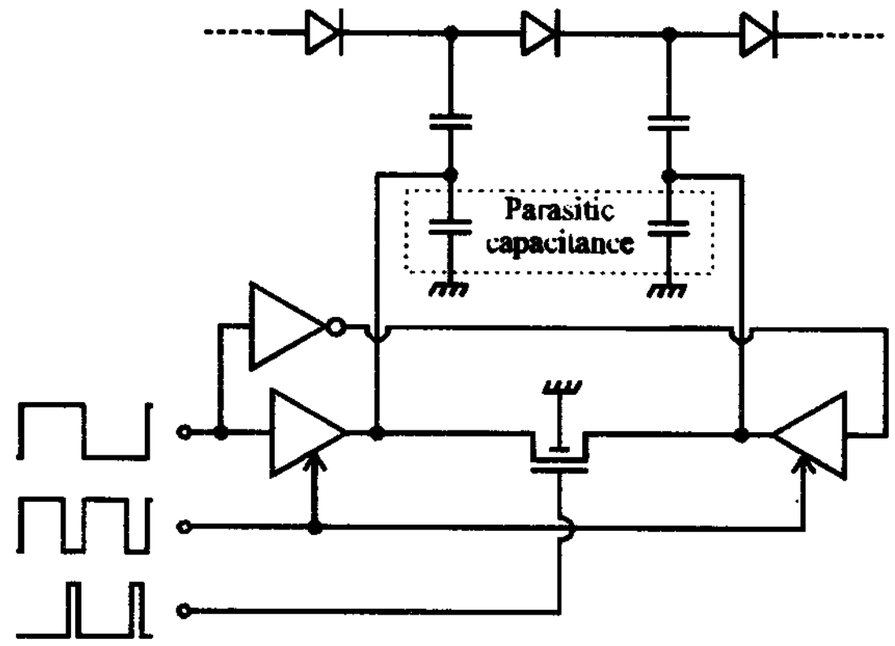

Figure 12: Principle of charge-recycling.

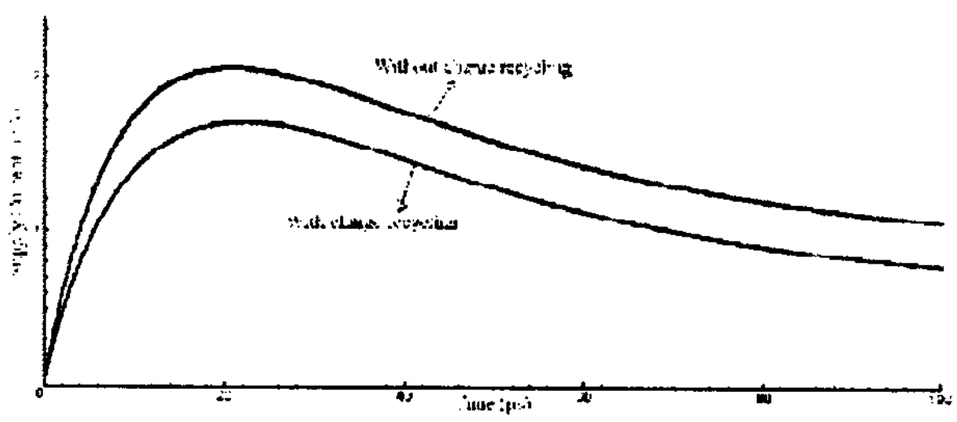

Figure 13: Simulation of the supply current reduction due to charge-recycling.

3. Conclusion

There is no doubt that the importance of bistable LCDs for portable battery-powered applications will grow considerably in the next years. There is, however, a lack of suitable low-power high-voltage driver chips for these displays at this moment. The programmable high-voltage generators presented in this paper have been designed and optimized specifically for driving bistable LCDs, and hence, they may contribute to a major breakthrough of bistable LCDs in the display market. Two very distinct classes of programmable high-voltage generators were discussed. A first type of high-voltage generator employs an external low-loss inductor and exhibits excellent electrical performance in terms of maximum output voltage and output current, as well as power efficiency, and hence, it is very suitable for most applications where the use of external passive components is allowed. If, however, a completely monolithic approach without external passive components is absolutely necessary, a second type of high-voltage generator with a fully integrated capacitor-based charge-pump can be chosen at the expense of a reduced output voltage and output current range and a lower power efficiency.

4. Acknowledgements

Part of the reported work has been carried out in the frame of the European projects HELICOS (Esprit #EP28131) and CARBINE (IST #2000-29450). The authors would like to thank the European Commission for their financial support.

5. References

[1] J. Doutreloigne, M. Vermandel, H. De Smet and A. Van Calster, "A micro-power 100V cholesteric texture LCD driver," in Proceedings of the SID International Symposium, pp. 328-331, (Baltimore, USA, May 2003).

[2] W. Hendrix, J. Doutreloigne and A. Van Calster, "Integrated low-power high-voltage driver for bistable nematic displays," in Proceedings of the SID International Symposium, pp. 376-379, (Seattle, USA, May 2004).